DOI 10.1007/s10511-018-9542-9
Astrophysics, Vol. 61, No. 3, September, 2018

HEATING OF INTERGALACTIC GAS NEAR GROWING BLACK HOLES DURING THE HYDROGEN REIONIZATION EPOCH

E. O. Vasiliev,[1] Yu. A. Shchekinov,[2,3] S. K. Sethi,[3] and M. V. Ryabova[4]

Black holes growing during Eddington accretion emit a large number of ultraviolet and x-ray photons which can influence the ionization and thermal state of the surrounding intergalactic gas before the onset of the hydrogen reionization epoch in the universe. This radiation heats the gas beyond the temperature of the relict radiation (cosmic microwave background CMB) $T_{CMB}(z)$ to a red shift $z \sim 8-12$ within 0.1-3 Mpc of a black hole with initial mass ~300 $M_\odot$ formed at z ~ 20-50 and growing with radiation efficiency $\varepsilon \sim 0.15-0.075$. The size of the gas regions in which the degree of ionization of hydrogen is higher than the residual value after recombination, i.e., greater than 10^{-4}, approaches the same levels. More substantial heating and ionization of the gas takes place in a smaller volume. In the vicinity of 30-300 kpc, for the same black hole parameters, it is heated to above 10^4 K or almost an order of magnitude greater than around a black hole with almost constant mass. The radiative flux from growing black holes is sufficient for complete (above 99%) production of ionized hydrogen and doubly ionized helium within 3-10 kpc of the parent minihalo. The recombination time for hydrogen in the ionization zones surrounding the black holes exceeds the local age of the universe for $z \lesssim 10$. These zones, which occupy several kiloparsecs, can become seeds for the next reionization of the universe. It turns out that extended regions with sizes of hundreds of kiloparsecs where radiation from growing black holes substantially changes the evolution of the intergalactic gas will radiate in the 21 cm line of

(1) Southern Federal University, Rostov-on-Don, Russia, Special Astrophysical Observatory, Russian Academy of Sciences, Russia, e-mail: eugstar@mail.ru
(2) P. N. Lebedev Physics Institute, Russian Academy of Sciences, Moscow, Russia, e-mail: yus@asc.rssi.ru
(3) Raman Research Institute, Bangalore, India, e-mail: sethi@rri.res.in
(4) Southern Federal University, Rostov-on-Don, Russia, e-mail: mryabova@sfedu.ru

Original article submitted February 27, 2018. Translated from Astrofizika, Vol. 61, No. 3, pp. 399-416 (August 2018).

atomic hydrogen, since the gas in these zones essentially remains neutral at a temperature exceeding that of the CMB.

Keywords: *reionization: black holes: accretion: x-ray radiation: intergalactic medium*

1. Introduction

The discovery of supermassive black holes $M \gtrsim 10^9 M_\odot$ at red shifts of $z \gtrsim 6$ [1,2] is an indication of the onset of seed formation for these objects at large red shifts with subsequent rapid growth of black holes (BH) during the epoch of the formation of the first stars, i.e., long before the onset of hydrogen reionization. Seeds of supermassive BH can be formed in various scenarios [3,4], one of which involves the collapse of massive first generation stars $M \sim 300 M_\odot$ [5-7] followed by growth of a BH through accretion of gas arriving during minihalo mergers [8-10]. Another possibility is the direct collapse of supermassive stars and the formation of BH with initial masses of $M \sim 10^5 M_\odot$ [11-16]. Leaving aside the question of the particular mechanism for formation of the seeds, we note that further growth of the BH is associated with effective accretion of gas, during which a substantial number of ultraviolet and x-ray photons are emitted. This ionizing radiation can clearly have a significant effect on the ionization and thermal state of the intergalactic gas surrounding the parent minihalo with the growing BH. It is assumed that the contribution of x-ray sources to the hydrogen reionization process is quite substantial [17-19], with the mass of the BH taken to be essentially constant. An increase in mass evidently leads to an increase in the size of the affected region surrounding isolated rapidly growing objects. Since these objects are definitely rare, but appear at larger red shifts, their observational manifestations may be more noticeable.

This paper is a detailed study of the ionization and thermal evolution of intergalactic gas in the vicinity of growing black holes during the epoch of the formation of the first objects. It is assumed that the seed BH are formed by collapse of massive stars. Thus, we limit ourselves to examining the first scenario for birth of black holes. The possible observational manifestations of growing BH will be examined separately. In the calculations we assume an ΛCDM model with parameters $(\Omega_m, \Omega_b, \Omega_\Lambda, h) = (0.29, 0.047, 0.71, 0.72)$. The model and its basic parameters are described in section 2, the results of the calculations are presented in section 3, and the main conclusions are given in section 4.

2. Description of the model

It is assumed that very massive first generation stars with masses $M \gtrsim 260 M_\odot$ collapse into BH [7]. These stars appear in the first protogalaxy-minihalos, which in terms of the hierarchical scenario for the development of high mass structures in the universe merge with one another to form more massive objects. It is these mergers into minihalos with the formation of black holes that supply the gas which facilitates the further growth of black holes during accretion and, as a result, leads to the appearance of BH with intermediate masses. During its evolution, the

mass M_{BH} of a BH can either remain almost constant without significant accretion or increase at the maximum accretion rate which ensures a maximal Eddington luminosity [20,21]:

$$M_{BH}(t) = M_{BH}(0)\exp\left(\frac{1-\varepsilon}{\varepsilon}\frac{t}{t_E}\right), \quad (1)$$

where $M_{BH}(0)$ is the initial BH mass, t_E = 0.45 billion years, ε is the radiation efficiency, which we assume equal to 0.1 in the calculations if no other value is specified, and the initial mass of the BH at red shift z_0 is $M_{BH} = 300\,M_\odot$. With an efficiency ε = 0.1, the mass of the BH increases by roughly a factor of 2500 over a time on the order of 400 million years. Raising ε to 0.2 leads to a significantly lower growth in mass, by roughly a factor of 33 over the same time, while lowering it to 0.05 enables growth by a factor of 1.5×10^7. Of course, such a large increase in the mass of an object requires a sufficient gas supply, which can be provided by mergers of minihalos. A high rate of mergers can evidently only occur in regions with a high concentration of minihalos. It is assumed that the first stellar objects, the precursors of the BH, are formed in minihalos with a total mass (including dark matter and baryons) of $M \sim 10^5 - 10^7\,M_\odot$ [22,23]. These minihalos appear at red shifts z ~ 20-50 in $(3-5)\sigma$ perturbations of the density field which are growing in the contemporary epoch in massive galaxies and clusters of them [24]. It is expected that during the formation of such minihalos, enough gas might be supplied in mergers for the rapid growth of massive BH [20]. For this reason, we shall consider the growth of BH formed at red shifts z ~ 20-50. Since we are studying the effect of rather rare objects on the surrounding gas, it seems important to limit the calculations to the epoch of the onset of hydrogen reionization, z ~ 8-10, so we assume that the evolutionary time for the BH is equal to 400 million years, which for an initial red shift z_0 = 20 corresponds to termination at $z \simeq 8.5$.

During accretion, a BH becomes a source of ultraviolet and x-ray radiation with a bolometric luminosity of $L_{BH} = 1.25\times10^{38}\,M_{BH}$ erg/s. We assume that the spectrum of the ionizing radiation has a power law dependence

$$L_\nu = L_0\left(\frac{h\nu}{I_H}\right)^\alpha, \quad (2)$$

where I_H is the ionization potential of hydrogen, α = -1.5, and L_0 is a normalization coefficient under the assumption that the BH radiates at energies from 13.6 to 10^4 eV.

Massive first generation stars which develop in a minihalo emit enough ionizing photons to strongly ionize the gas inside the minihalo [25-27] and enable the escape of photons from the parent minihalo. The BH formed from these stars emit ionizing photons which can leave the minihalo and participate in ionization of the surrounding intergalactic matter. Thus, the spectral flux of radiation at distance *r* from a BH inside a minihalo will be given by

$$F_\nu = \frac{L_\nu}{4\pi r^2}\exp(-\tau_h)\exp(-\tau_{IGM}), \quad (3)$$

where the first exponential factor is associated with absorption in the parent minihalo, with $\tau_h \sim N_{\rm HI}^h$, where $N_{\rm HI}^h$ is the HI column density inside the minihalo and this quantity is assumed constant in the calculations. The second exponential factor is determined by absorption in the surrounding gas and depends on its ionization history, which is described below. In general, there is a transition region between the minihalo and the surrounding intergalactic gas with a complicated distribution of density, temperature, and velocity of the gas. Because of the strong flux of ionizing radiation, however, we can assume that the gas is almost fully ionized; in addition, the size of this region is comparable to the virial radius of the minihalo and the density in it is considerably lower than in the halo, so that the contribution to the total absorption from this region will be minimal. Thus, we can begin the calculations for the background gas outside the parent minihalo. We assume for simplicity that the background gas is distributed uniformly and its density varies as $\sim (1+z)^3$ while its temperature varies as $\sim (1+z)^2$.

We consider the ionization and thermal evolution of the gas in concentric spherical shells centered at the location of the BH. The radii of the shells lie in a range from 10^3 to 10^7 pc, and the radii of neighboring shells differ by a factor of $a_r = 1.1$, so that $r_{i+1} = a_r r_i$. The total number of shells for this range of distances is about 100. Note that the radius of the inner shell is roughly a factor of three greater than the virial radius of a minihalo with total mass $M = 10^7\, M_\odot$ formed at $z = 20$ [28].

The system of equations for the ionization kinetics and thermal evolution of a hydrogen-helium plasma was solved for each spherical region. These equations include all the basic processes taking place in the material in its initial chemical state, in particular, collisional ionization and recombination for HI, HII, HeI, HeII, HeIII and , photoionization by ultraviolet and x-ray radiation from the BH, and absorption both inside the protogalaxy and by the background intergalactic gas. The equation for the temperature includes cooling processes owing to collisional ionization of HI, HeI, and HeII, recombination of HII and HeII (both radiative and dielectronic), and HeIII, collisional excitation of HI, HeI (1^2S and 2^3S), and HeII, free-free transitions, and heating owing to the Compton process, and photoionization. The chemical reaction rates and cooling/heating rates are taken from Refs. 29 and 30. Since we are discussing x-ray ionization, the effect of secondary electrons must be included [31,32]. The temperature equation must also include a term for adiabatic cooling owing to Hubble expansion of the universe, since we are considering the evolution of the background gas over times exceeding the local age of the universe. The initial temperature and degree of ionization of the hydrogen for a given red shift were calculated using the RECFAST program [33]. Helium was assumed to be initially completely neutral.

3. Ionization and thermal evolution of the gas

We mostly examine the evolution of the intergalactic gas surrounding a minihalo with a BH of constant mass and in the case of a BH that grows because of efficient accretion. Figure 1 shows the radial profiles of temperature and of the number densities of hydrogen and helium ions surrounding a minihalo with black holes of constant and increasing mass which begin to radiate efficiently at a red shift of $z_0 = 20$. It can be seen that by a red shift $z = 16.5$, i.e., after almost 55 million years, the gas has been heated above 10^4 K inside a sphere of radius ~300-400 pc, both

around the BH with a fixed mass of $M_{BH} = 300\,M_{\odot}$ and around a BH with an initial mass of $M_{BH} = 300\,M_{\odot}$ and a radiation efficiency of ε = 0.1. The small difference is related to the fact that over this time the mass of the growing BH has stayed fairly close to its initial value, having increased precisely by only a factor of 3. Over the next 100 million years (from z = 16.5 to 12.5), the difference in the radii of the regions occupied by the hot gas increases and reaches almost an order of magnitude. By a red shift of z = 8.5, i.e., by 400 million years, the radius of the region around the constant mass BH has increased to almost 10 kpc, while the hot gas has spread by more than 100 kpc

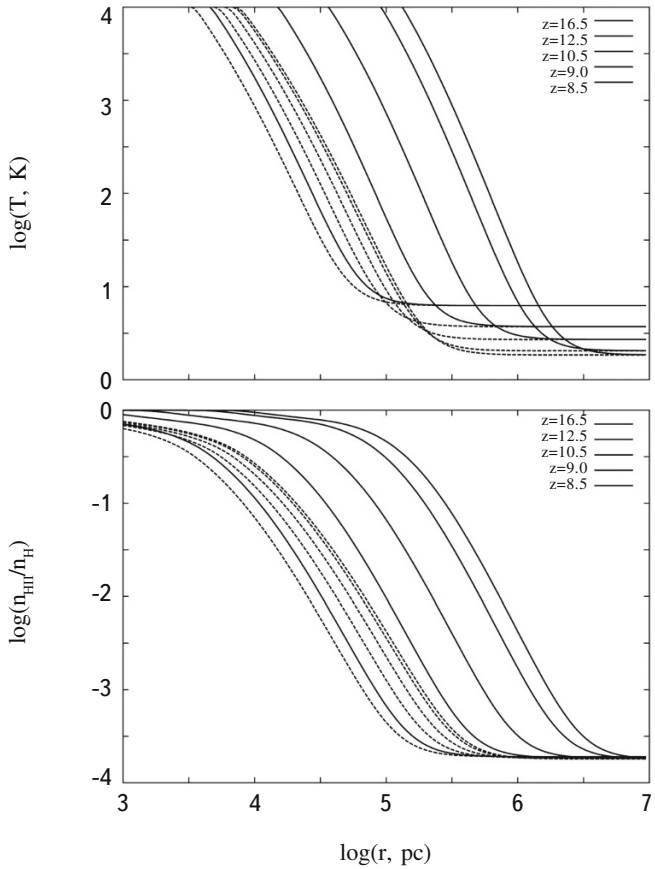

Fig. 1. Radial distributions of the temperature (top frame), and fractions of HII (upper middle frame), HeII (lower middle frame), and HeIII (bottom frame) around a growing BH which begins evolving at $z_0 = 20$ for times z = 16.5, 12.5, 10.5, 9, and 8.5 (curves from left to right). The dashed curves correspond to the evolution of a BH with a constant mass $M_{BH} = 300\,M_{\odot}$ and the smooth curves show the evolution of a growing BH with initial mass $M_{BH}(z = z_0) = 300\,M_{\odot}$ and radiation efficiency ε = 0.1.

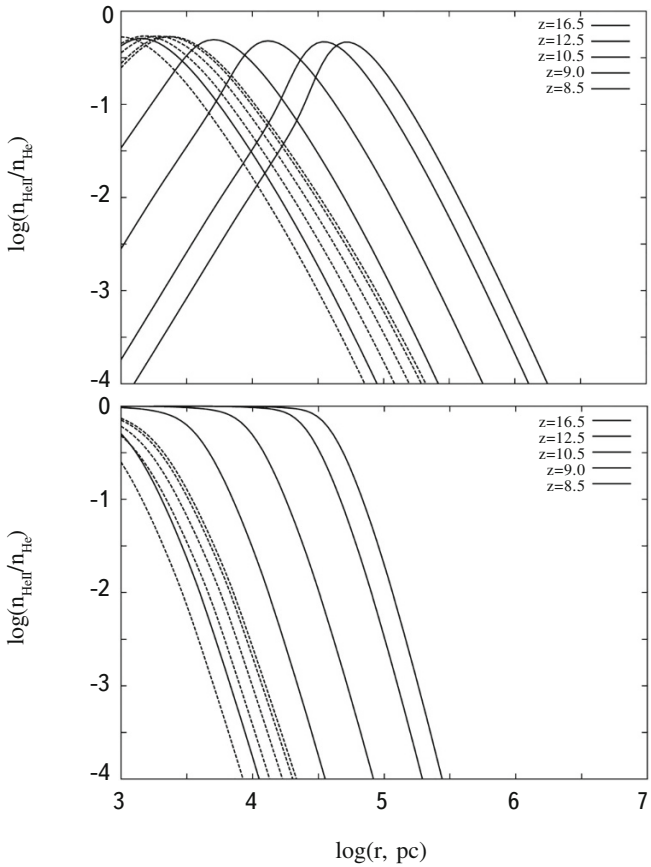

Fig. 1. Conclusion

around the growing BH. By this time the mass of the BH has grown by a factor of 2500.

The radiation from the BH both heats and ionizes the surrounding intergalactic gas, which by a red shift of $z \lesssim 100$ turns out to be almost neutral with a residual degree of ionization for the hydrogen of ~10^{-4} and completely neutral helium. It can be seen in the second frame from the top in Fig. 1 that the degree of ionization of hydrogen is close to 1 within a sphere of radius ~1-10 kpc in the vicinity of a stationary as well as a growing BH. Note that the degree of ionization around a growing BH is systematically higher than that around a BH with a fixed mass. Thus, in the case of a growing BH, by z = 8.5 the hydrogen is fully ionized within a sphere of radius ~10 kpc. In general, the presence of a BH leads to differences in the degree of ionization from the background residual value within a much larger volume of up to 200-300 kpc for a BH with a constant mass of $M_{BH} = 300\,M_{\odot}$ and by an order of magnitude greater in the case of a growing BH with an initial mass of $M_{BH} = 300\,M_{\odot}$ and a radiation efficiency of $\varepsilon = 0.1$.

The existence of far ultraviolet and soft x-ray photons in the spectrum supports efficient ionization of helium, as can be seen clearly in the two bottom frames of Fig. 1. It is to be noted that in the vicinity of a BH with a constant mass, helium is in roughly equal amounts of states HeII and HeIII. This region of ionized helium extends to ~3 kpc.

In the case of a growing BH with an initial mass of $M_{BH} = 300\,M_{\odot}$ and a radiation efficiency of ε = 0.1, by the time z = 8.5 the zone of fully ionized helium HeIII extends to 20 kpc and the fraction of singly ionized HeII reaches maximum values of order 0.5 at a distance of ~50 kpc. Thus, growing black holes change the ionization and thermal state of the surrounding intergalactic gas significantly.

We now examine how this influence of black holes depends on the initial red shift and mass of the BH. Figure 2 shows the radial distributions of the temperature and the fractions of the HII, HeII, and HeIII ions around a growing

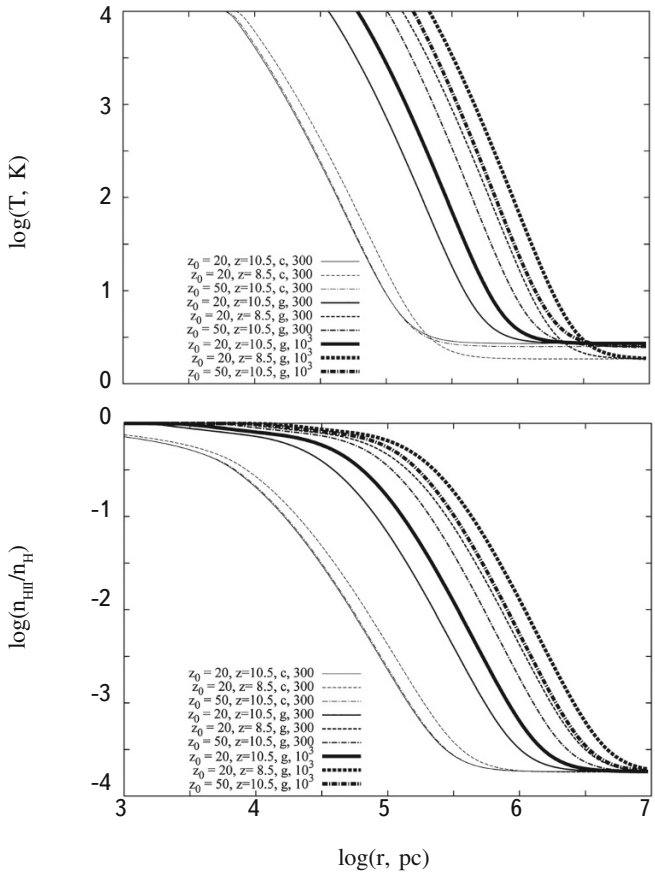

Fig. 2. Radial distributions of the temperature (top frame), and fractions of HII (upper middle frame), HeII (lower middle frame), and HeIII (bottom frame) around growing black holes for which evolution begins at z_0 = 20 and 50 for times z = 10.5 and 8.5. The thin curves correspond to the evolution of a BH with constant (labeled "c") mass $M_{BH} = 300\,M_{\odot}$, the thicker curves show the evolution of a growing BH with an initial mass $M_{BH}(z = z_0) = 300\,M_{\odot}$, and the thickest curves correspond to the evolution of BH with an initial mass $M_{BH}(z = z_0) = 300\,M_{\odot}$. The radiation efficiency for the growing black holes was taken to be ε = 0.1.

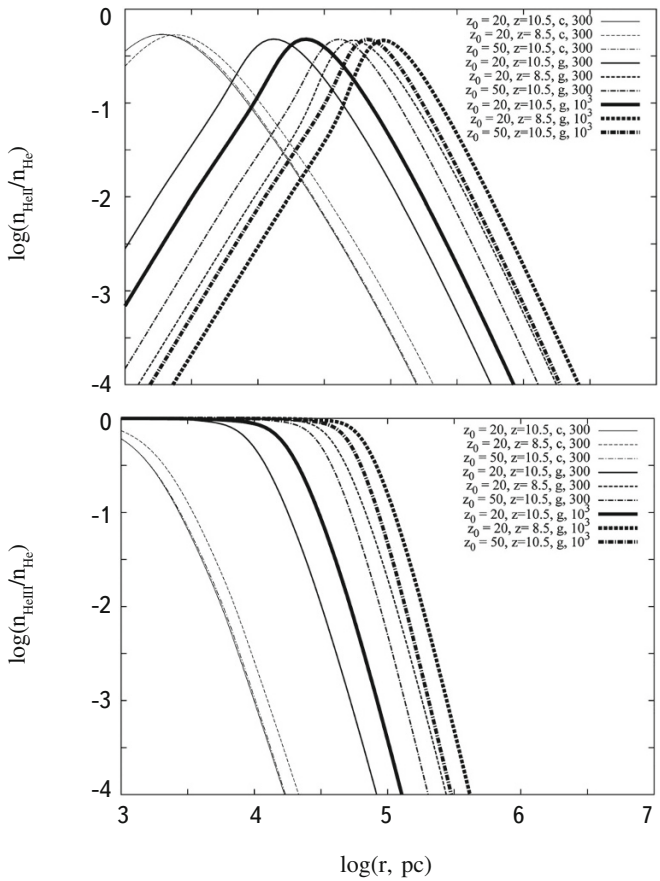

Fig. 2. Conclusion

BH, the evolution of which began at z_0 = 20 and 50 at the times when z = 10.5 and 8.5 for a BH with a constant (labeled "c") mass $M_{BH} = 300\,M_\odot$ and for growing BH with initial masses $M_{BH}(z = z_0) = 300\,M_\odot$ and $10^3\,M_\odot$. The radiation efficiency for the growing BH is ε = 0.1. We note that the masses of the growing BH formed at z_0 = 20 and 50 reach the same level, roughly 2500 times greater than the initial value, by red shifts of 8.5 and 10.5, respectively. It can be seen clearly that the size of the zone of hot and ionized gas depends weakly on the time the evolution of the BH begins, with differences of up to 5-20% (compare the dashed and dot-dashed curves of similar thickness). An increase in the initial mass of the BH to $10^3\,M_\odot$ leads to a more substantial rise in the radius of the zone – by almost a factor of 1.5 by the time of a red shift of 8.5.

The substantial difference between the sizes of the zones surrounding black holes with constant and growing masses can be seen easily in Figs. 1 and 2. Thus, it is the accretion rate and the radiation efficiency ε which are responsible for these large differences. When ε is higher, the growth in mass of the BH is small according to Eq. (1); e.g., over 400 million years for ε = 0.3 the mass increases by roughly a factor of 7.5, and for ε = 0.2, a factor of 33. Since a significant increase in the mass takes place only in the last 50-100 million years, substantial variations in the enlargement of the ionization zone are to be expected if the final mass of the BH will differ from the initial

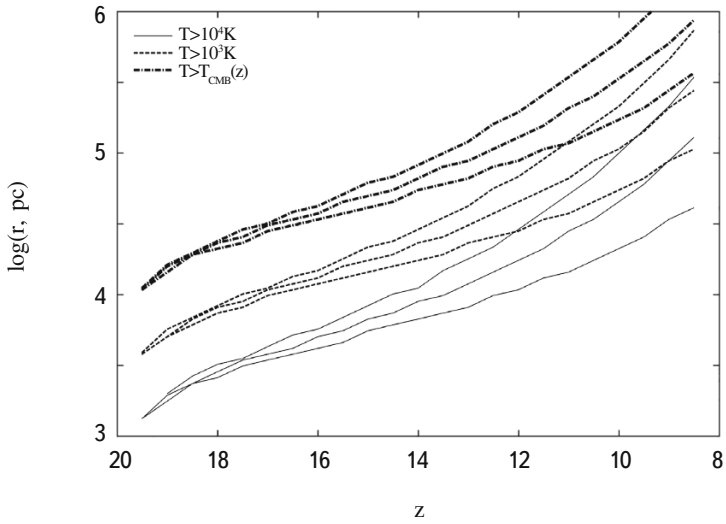

Fig. 3. The radii of the spherical regions surrounding BH within which the gas temperature exceeds 10^4 K (solid curves), 10^3 K (dashed curves) and $T_{CMB}(z)$ (dotted curves) for BH which began to grow at $z_0 = 20$ with an initial mass of $M_{BH}(z = z_0) = 300\,M_\odot$ and radiation efficiencies $\varepsilon = 0.075$, 0.1, and 0.15 (top to bottom).

mass by more than a factor of 100. For this reason, in the following we examine the evolution of black holes with radiation efficiencies $\varepsilon \lesssim 0.15$.

We now consider in more detail the evolution of the heated and ionized intergalactic gas in the vicinity of a minihalo with a growing BH. Figure 3 shows the evolution of the size of the spherical regions surrounding a BH within which the gas temperature exceeds a certain limit: 10^4 K (solid curves), 10^3 K (dashed curves), and $T_{CMB}(z)$ (dotted curves), for black holes which begin to grow at $z_0 = 20$ with an initial mass of $M_{BH}(z = z_0) = 300\,M_\odot$ and radiation efficiencies of ε = 0.075, 0.1, and 0.15 (curves of each type from the top downward, respectively). It is clear that for $z \gtrsim 17$ the size of the regions of heated gas are almost independent of ε and only for smaller red shifts do the differences become noticeable. Toward the end of the calculations at z = 8.5, the radii of the regions heated above the specified temperature differ by almost an order of magnitude for ε = 0.15 and 0.075, regardless of the temperature limit. Again it should be pointed out that the final sizes of the regions lie within an interval from several tens to hundreds of kpc. This is comparable to or larger than the characteristic distances between minihalos in which star formation is possible. Thus, other minihalos whose evolution may be affected by radiation from a BH can appear in the zones of influence surrounding growing black holes [17].

For growing BH whose evolution begins at large red shifts, the heated gas zones are larger if their size is considered at the same red shift. For example, at $z \simeq 11$ the region with $T > 10^4$ K for a BH formed at $z_0 = 50$ is almost an order of magnitude larger than for a BH whose evolution began at $z_0 = 20$ (see the solid curves in Fig. 4;

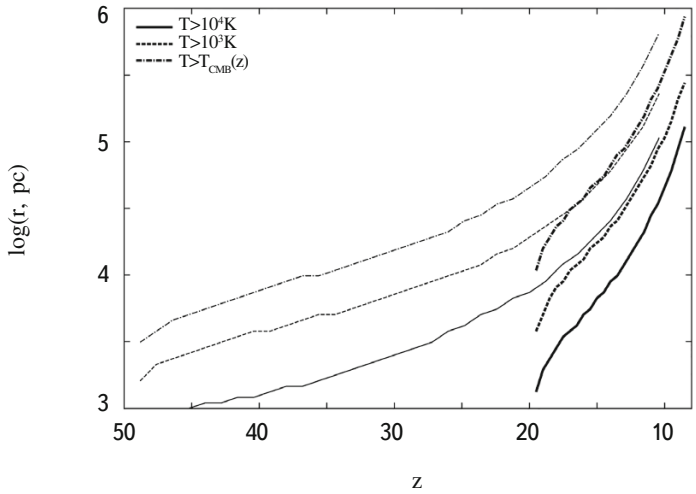

Fig. 4. The radii of the spherical regions surrounding BH within which the gas temperature exceeds 10^4 K, 10^3 K, and $T_{CMB}(z)$ (solid, dashed, and dot-dashed curves from bottom to top, respectively) for BH that begin to grow at $z_0 = 20$ (thick curves) and 50 (thin curves) with initial mass $M_{BH}(z = z_0) = 300\,M_\odot$ and radiation efficiency $\varepsilon = 0.1$.

the top curve corresponds to $z_0 = 50$ and the bottom curve, to $z_0 = 20$). Subsequently, with a retained accretion rate the size of the zone surrounding the latter even exceeds the radius of the region surrounding a BH which began to evolve earlier. This circumstance is important for evaluating the filling factor of the intergalactic gas subjected to the radiation from growing black holes.

The transition to larger red shifts means a significantly smaller number of minihalos in which a star population and black holes can be formed. These halos correspond to (5-6)σ fluctuations in the density field at $z \sim 50$, while at $z \sim 20$ these minihalos develop from substantially less rare (3-4)σ fluctuations. Thus, the filling factor for the gas subject to the influence of radiation from growing black holes will be determined by objects that began to evolve shortly before the red shift being examined. More precisely, these are growing BH with $\varepsilon \lesssim 0.15$, which began to evolve roughly 300 million years before the red shift of interest to us. Indeed, after 200-300 million years the mass of the BH begins to grow exponentially. For example, at a red shift of $z \sim 10$, the contribution from growing black holes formed at $z_0 = 20$ will predominate.

The almost full ionization (above 99%) near the galactic gas in the neighborhood of growing black holes is an important fact. Here the helium can be doubly ionized (Figs. 1-2). Figure 5 shows the evolution of the radius of the spherical regions surrounding BH within which the relative concentration of HII ions (thick curves) or HeIII ions (thin curves) exceeds 0.99 for BH which began to grow at $z_0 = 20$, 30, and 50 (solid, dashed, and dotted curves, respectively) with an initial mass of $M_{BH}(z = z_0) = 300\,M_\odot$ and radiation efficiency $\varepsilon = 0.1$. It should be noted, first

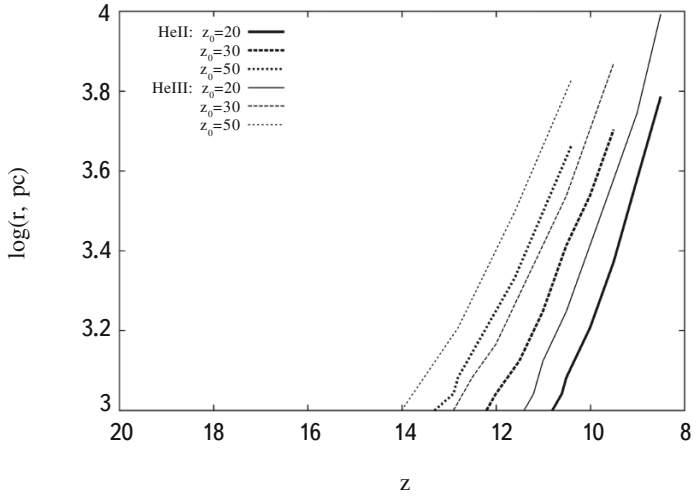

Fig. 5. Radii of the spherical regions surrounding BH within which the relative concentration of HII ions (thick curves) or HeIII ions (thin curves) exceeds 0.99 and which began growing at $z_0 = 20$, 30, and 50 (solid, dashed, and dotted curves, respectively) with initial mass $M_{BH}(z = z_0) = 300\,M_\odot$ and radiation efficiency $\varepsilon = 0.1$.

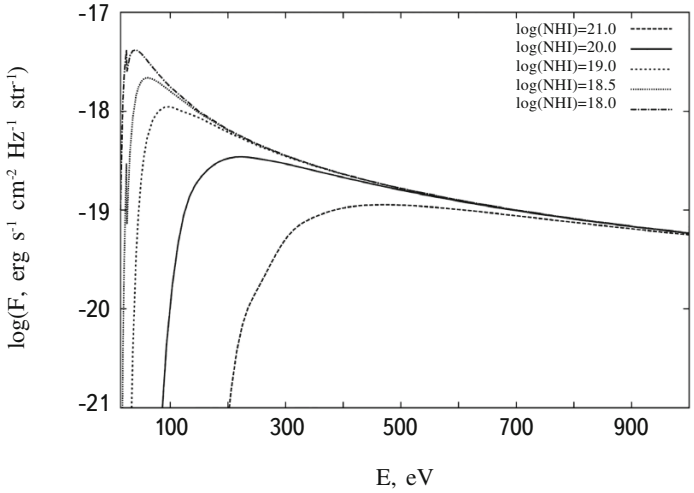

Fig. 6. Spectrum of ionizing radiation leaving a parent minihalo at a distance of 1 kpc for several values of the HI column density, $\log[N_{HI}, \mathrm{cm}^{-2}] = 18$, 18.5, 19, 20, and 21, for BH that begin to grow at $z_0 = 20$ with initial mass $M_{BH}(z = z_0) = 300\,M_\odot$ and radiation efficiency $\varepsilon = 0.1$.

of all, that the ionization zones are considerably smaller than the regions in which the gas temperature exceeds 10^4 K, and they increase more rapidly (Fig. 5) than the size of the heated gas regions (Fig. 4). Second, the HeIII ionization zones are somewhat larger than the HII ionization zones, because ionization is predominantly by photons with energies greater than 100 eV (Fig. 6), for which the HeII ionization cross section is greater than that for HI. In fact, since it is assumed that the column density of neutral hydrogen inside a minihalo is nonzero and is taken to be $N_{HI} = 10^{20}$ cm^{-2} in the calculations, photons with energies of 13.6-100 eV are absorbed inside the minihalo and only the more energetic photons escape outward. When the column density N_{HI} is lower, absorption inside the parent minihalo becomes weaker (Fig. 6) and the positions of the HeII and HI ionization fronts essentially coincide at N_{HI} ~ $10^{18.5}$ cm^{-2}, and for lower $N_{\rm HI} \lesssim 10^{18}$, the size of the HI zone exceeds or is the same as that of the HeIII zone (Fig. 7).

Since hydrogen and helium ionization zones develop around growing black holes, these objects can contribute to the reionization of hydrogen and, possibly, even of helium. Thus, it is interesting to estimate the lifetime of the zones after possible cessation of a significant flux of ionizing photons owing to reduced accretion. Figure 8 shows the recombination time in the HII and HeIII ion zones. It is clear that for $z \lesssim 10$ the recombination time for hydrogen inside these zones is greater than the local age of the universe; thus, these zones are probably conserved even after

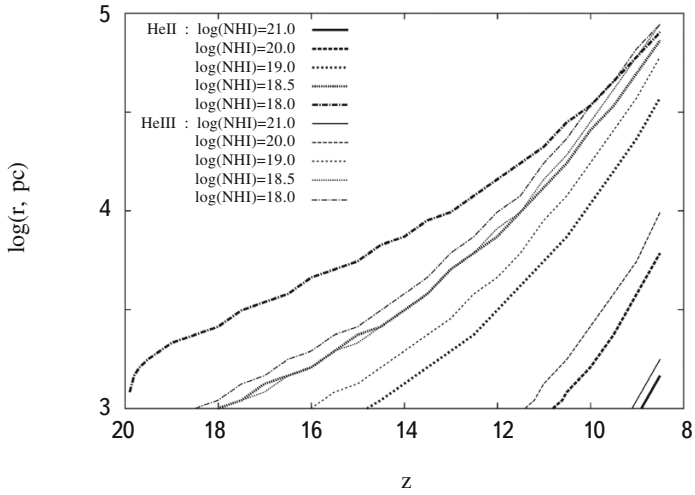

Fig. 7. Radii of the spherical regions surrounding BH within which the relative concentration of HII ions (thick curves) or HeIII ions (thin curves) exceeds 0.99 and which began growing at $z_0 = 20$, 30, and 50 (solid, dashed, and dotted curves, respectively) with initial mass $M_{BH}(z = z_0) = 300\,M_\odot$ and radiation efficiency $\varepsilon = 0.1$, for several values of the column density HI in the parent minihalo, log[N_{HI}, cm^{-2}] = 18, 18.5, 19, 20, and 21.

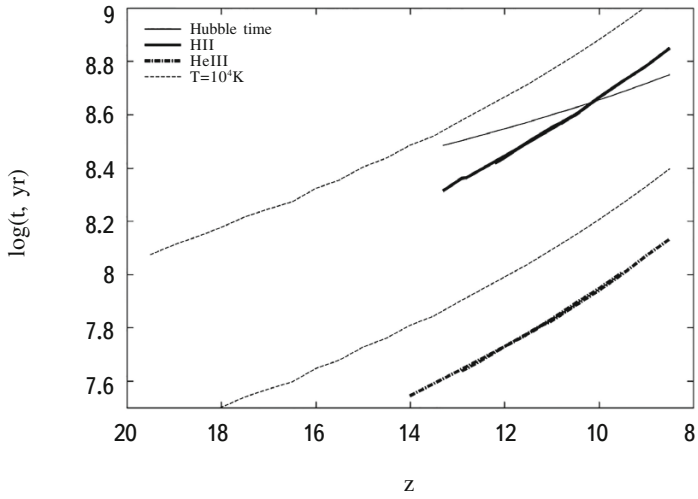

Fig. 8. The recombination time for hydrogen HII (thick, solid curves) and helium HeIII (thick, dot-dashed curves) inside spherical zones surrounding black holes within which the fractions of HII or HeIII exceed 0.99 for BH that began growing at z_0 = 20, 30, and 50 (thick curves superimposed on one another) with an initial mass $M_{BH}(z = z_0) = 300\,M_\odot$ and radiation efficiency ε = 0.1. The thin dashed curves correspond to the recombination time for HII (top) and HeIII (bottom) for gas with a temperature of $T = 10^4$ K. The thin smooth curve shows the age of the universe (the local Hubble time).

a BH "shuts down." Here the recombination time for helium HeIII is considerably, by more than a factor of 3, shorter than the Hubble time; i.e., HeIII recombines rapidly. Here the helium remains singly ionized and this may be the start of its reionization. It should be noted that the recombination time for hydrogen in the less cold gas with $T \sim 10^4$ K, which extends over substantially larger distances, becomes longer than the Hubble time at approximately $z \lesssim 14$, which facilitates the conservation of extended, partially ionized regions with a high fraction of neutral hot gas, which could be detected as emission in hyperfine structure lines of atomic hydrogen.

4. Conclusion

During Eddington accretion onto black holes a large amount of ultraviolet and x-ray photons are emitted which can ionize and heat the surrounding medium. In this paper we have studied the influence of this ionizing radiation from growing black holes in the first minihalos (protogalaxies) on the state of the surrounding intergalactic gas up to the start of the hydrogen reionization epoch. It has been shown that:

– radiation from growing black holes changes the thermal state of the intergalactic gas within a large volume.

In particular, the gas is heated to above the temperature $T_{CMB}(z)$ of the cosmic background inside a volume with a radius of 0.1-3 Mpc to a red shift of z ~ 8-12 during accretion with radiation efficiency $\varepsilon \sim 0.15-0.075$ onto a black hole with initial mass ~$300\,M_\odot$ formed at red shifts of z ~ 50-20;

– the intergalactic gas in the vicinity of minihalos with growing black holes with a radiation efficiency $\varepsilon \lesssim 0.15$ for 300-400 million years is heated to temperatures above 10^4 K within a region with a radius on the order of 30 kpc; increasing the accretion rate to $\varepsilon \lesssim 0.075$ causes the heating region to expand by an order of magnitude, to 300 kpc; for weak accretion, i.e., an insignificant change in the (almost constant) mass of the black hole, the size of the hot gas region only reaches 5-8 kpc;

– the gas regions in which the degree of ionization of hydrogen is higher than the residual level after recombination, i.e., above ~10^{-4}, reach a size of 0.3-3 Mpc around growing black holes with radiation efficiencies $\varepsilon \lesssim 0.15-0.075$ and initial masses $\sim 300-10^3\,M_\odot$ formed at red shifts of z ~ 50-20. The radiative flux from these black holes is sufficient to fully (above 99%) ionize hydrogen and doubly ionize helium within 3-10 kpc from the parent minihalo. Here the order of the ionization fronts for HII and HeIII depends on the absorption of radiation in the parent galaxy: for a column density $N_{\rm HI} \gtrsim 10^{18.5}$ cm^{-2}, the HeIII ionization front precedes that for HII, because of the absorption of ultraviolet photons with energies of 13.6-100 eV in the parent minihalo and ionization of the intergalactic gas predominantly by soft x-ray photons, for which the cross section for ionization of HeII is greater than that for HI, while for a lower $N_{\rm HI} \lesssim 10^{18}$ cm^{-2} the HI zone, as expected, is larger than or the same size as the HeIII zone.

The large changes in the ionization and thermal state of the intergalactic gas in the vicinity of growing black holes is indicative of a contribution to the reionization of the universe, since the recombination time for hydrogen in the ionization zones surrounding black holes exceeds the local age of the universe for $z \lesssim 10$. These zones, which occupy a few kiloparsecs, can become seeds for subsequent reionization of the universe, as the regions in which the evolution of the intergalactic gas changes significantly owing to the radiation from growing black holes, i.e., the gas is ionized and heated, extend for hundreds of kiloparsecs, or substantially more than the average distance between minihalos, which is a few tens of kiloparsecs for red shifts z ~ 10-15. Thus, a single rapidly growing black hole can influence the ionization state of a substantial volume of surrounding space. Since the gas in this volume is substantially neutral and its temperature exceeds that of the background radiation, it turns out that this gas will radiate in the 21 cm atomic hydrogen line at a radiative flux that may be sufficient for detection by the LOFAR, MWA, and SKA radiointerferometry arrays [34].

This work was supported by a joint Russian-Indian RFBR-DST project (project RFFI 17-52-45063_IND, project DST P-276). The program package for modelling the thermal evolution was developed with the support of the Russian Science Foundation (project 14-50-00043). The work of Yu. A. Shch. was supported by program No. 28 of the Presidium of the Russian Academy of Sciences. The work of M. V. R. was partially supported by the Ministry of Education and Science of Russia (project 3.858.2017/4.6).

REFERENCES

1. D. J. Mortlock, et al., Nature, **474**, 616 (2011).
2. X.-B. Wu, et al., Nature, **518**, 512 (2015).
3. Z. Haiman, in: T. Wiklind, B. Mobasher, and V. Bromm, eds., The First Galaxies, Astrophys. Space Sci. Library, **396** (2013), p. 293.
4. M. Volonteri, Science, **337**, 544 (2012).
5. N. Yoshida, K. Omukai, and L. Hernquist, Science, **321**, 669 (2008).
6. A. Stacy, T. H. Greif, and V. Bromm, Mon. Not. Roy. Astron. Soc. **422**, 290 (2012).
7. S. E. Woosley and A. Heger, Very Massive Stars in the Local Universe, Astrophys. Space Sci. Library, **412**, 199, (Springer International Publishing) (2015).
8. P. Madau and M. J. Rees, Astrophys. J. **551**, L27 (2001).
9. Z. Haiman and A. Loeb, Astrophys. J. **552**, 459 (2001).
10. M. Volonteri, F. Haardt, and P. Madau, Astrophys. J. **582**, 559 (2003).
11. A. Loeb and F. A. Rasio, Astrophys. J. **432**, 52 (1994).
12. S. P. Oh and Z. Haiman, Astrophys. J. **569**, 558 (2002).
13. G. Lodato and P. Natarajan, Mon. Not. Roy. Astron. Soc. **371**, 1813 (2006).
14. K. Inayoshi, K. Omukai, and E. Tasker, Mon. Not. Roy. Astron. Soc. **445**, L109 (2014).
15. F. Becerra, T. H. Greif, V. Springel, et al., Mon. Not. Roy. Astron. Soc. **446**, 2380 (2015).
16. M. A. Latif, D. R. G. Schleicher, and T. Hartwig, Mon. Not. Roy. Astron. Soc. **458**, 233 (2016).
17. Z. Haiman, T. Abel, and M. J. Rees, Astrophys. J. **534**, 11 (2000).
18. M. Ricotti and J. P. Ostriker, Mon. Not. Roy. Astron. Soc. **352**, 547 (2004).
19. M. B. Eide, L. Graziani, B. Ciardi, et al., Mon. Not. Roy. Astron. Soc. **476**, 1174 (2018).
20. M. Volonteri and M. J. Rees, Astrophys. J. **633**, 624 (2005).
21. M. Volonteri and M. J. Rees, Astrophys. J. **650**, 669 (2006).
22. Z. Haiman, A. A. Thoul, and A. Loeb, Astrophys. J. **464**, 523 (1996).
23. M. Tegmark, J. Silk, M. J. Rees, et al., Astrophys. J. **474**, 1 (1997).
24. L. Gao, S. D. M. White, A. Jenkins, et al., Mon. Not. Roy. Astron. Soc. **363**, 379 (2005).
25. D. Whalen, T. Abel, M. L. Norman, Astrophys. J. **610**, 14 (2004).
26. T. Kitayama, N. Yoshida, H. Susa, et al., Astrophys. J. **613**, 631 (2004).
27. E. O. Vasiliev, E. I. Vorobyov, A. O. Razoumov, et al., Astron. Rep. **56**, 564 (2012).
28. B. Ciardi and A. Ferrara, Spa. Sci. Rev. **116**, 625 (2005).
29. R. Cen, Astrophys. J. Suppl. Ser. **78**, 341 (1992).
30. S. C. O. Glover and A.-K. Jappsen, Astrophys. J. **666**, 1 (2007).
31. M. Ricotti, N. Y. Gnedin, and J. M. Shull, Astrophys. J. **575**, 33 (2002).

32. J. M. Shull and M. E. van Steenberg, Astrophys. J. **298**, 268 (1985).

33. S. Seager, D. Sasselov, and D. Scott, Astrophys. J. Supll. Ser. **128**, 407 (2000).

34. E. O. Vasiliev, Sh. K. Sethi, and Yu. A. Shchekinov, Astrophys. J., submitted (2018).